POLITECNICO DI TORINO
Repository ISTITUZIONALE

A probabilistic approach for the evaluation of the stabilizing forces of fully grouted bolts

(Article begins on next page)

18 April 2024

A probabilistic approach for the evaluation of the stabilizing forces of fully grouted bolts

Pierpaolo Oreste[1], Giovanni Spagnoli[2]*

[1] Department of Environmental, Land and Infrastructure Engineering, Politecnico di Torino, Corso Duca Degli Abruzzi 24, 10129 Torino, Italy, *pierpaolo.oreste@polito.it*

ORCID: 0000-0001-8227-9807

[2] MBCC Group, Dr-Albert-Frank-Strasse 32, 83308 Trostberg, Germany,

*corresponding author, Tel: +49 8621 86-3702, *giovanni.spagnoli@mbcc-group.com*

ORCID: 0000-0002-1866-4345

Abstract

The essential task of the ground reinforcement techniques is to keep the rock as stable as possible. In particular passive rock bolt should resist the rock movements along its entire length and through the resulting reaction forces, to improve the load-bearing capacity of the rock. Among different calculation techniques, the calculations based on Block Reinforcement Procedure (BRP) was used in this paper, also adopting some simplified equations available in the scientific literature. However, parameters influencing the interaction are difficult to evaluate. Therefore, the problem of the reliable definition of the parameters that most influence the behavior of the bolts and the evaluation of the stabilizing forces of the potentially unstable block of rock remains. A new probabilistic approach is presented in this article, able to appropriately manage the uncertainties present on the fundamental parameters of the bolt-rock interaction and on the mechanical characteristics of the sliding surface of the block. Through the use of a Monte Carlo procedure, in fact, it was possible to obtain different samples of

the safety factors of the rock block, one for each diameter of the steel bars used for its

stabilization. Finally, the probabilistic management of the safety factor samples

allowed the correct design of the steel bars, by evaluating the probability that the safety

factor of the block with regard to potential slipping has a value lower than a pre-

established limit. The probabilistic approach developed was applied to a real problem

of stabilization of a potentially unstable rock block due to planar sliding, present on a

municipal road in North Italy.

Keywords: rock bolt; Winkler spring approach; rock block stabilisation; safety factor;

Monte Carlo simulation, probabilistic approach,

Abbreviations and nomenclature

35 A Area of the sliding surface of the block;

36 A_{bar} Area of the section of the steel bar constituting the bolt

37 c Cohesion on the natural discontinuity which constitutes the sliding

38 surface;

39 $(EA)_{bolt}$ Axial stiffness of the bolt

40 E_{binder} Elastic modulus of the binder surrounding the steel bar in the hole

41 $(EJ)_{bolt}$ Bending stiffness of the bolt

42 E_{st} Steel elastic modulus

43 $f(x)$ Probability density associated with the x value of the geotechnical or

44 geomechanical parameter considered;

45 F_S Safety factor;

46 J_{bar} Moment of inertia of the steel bar constituting the bolt

47 k Ratio between the normal pressure, p, which is applied on the perimeter

48 of the bolt (on the wall of the hole) by the surrounding rock and the

49 normal displacements, y, of the bolt

50 L_a Bolt length inside the unstable block

51 L_p Bolt length in the stable rock behind the unstable block

52 L_{test} Length of the tested bolt

53 M Bending moment in the bolt

54 N Axial force in the bolt

55 $N_{0,\delta_{max}}$ Bolt stabilising force in the direction of the bolt axis

56 N_{test} Tensile axial force applied at the bolt head from pull-out tests

57 N_{yield} Force causing the bar failure under tensile stress

58 N_{slip} Force causing the bolt-rock interface to fail for a unit bolt length

59	N_0	Value of the tensile force in the axial direction of the bolt on the
60		intersection point between the bolt and a block surface
61	n	Number of fully grouted passive bolts present;
62	T	Shear force in the bolt
63	t_{binder}	Thickness of the binder annulus surrounding the steel bar
64	T_0	Value of the shear force perpendicular to the axial direction of the bolt
65		on the intersection point between the bolt and a block surface
66	$T_{0,\delta_{max}}$	Bolt stabilising force in the transverse direction
67	v_r	Value of the relative axial displacement between the bolt and the
68		surrounding rock
69	W	Weight of the potentially unstable rock block;
70	y	Normal displacements of the bolt perpendicular to the axial direction of
71		the bolt
72	α	Parameter characterising the interaction in the axial direction between
73		the bolt and the surrounding rock $\alpha = \sqrt{\dfrac{\beta_c \cdot P_{hole}}{EA}}$
74	β	Parameter characterizing the interaction in the transverse direction
75		between the bolt and the surrounding rock $\beta = \sqrt[4]{\dfrac{k \cdot \Phi_{hole}}{4 \cdot EJ}}$
76	β_c	Ratio between the shear stresses, τ, that develop on the perimeter of the
77		bolt and the relative axial displacements, v_r
78	δ_{max}	Maximum displacement component of the block in the axial direction of
79		the bolt
80	φ	Friction angle on the natural discontinuity constituting the sliding surface
81	Φ_{bar}	Diameter of the steel bar
82	Φ_{hole}	Diameter of the hole (of the bolt)

83   μ Mean value of the distribution;

84   χ Adimensional parameter for the evaluation of the stabilising forces

85   λ Adimensional parameter for the evaluation of the stabilising forces

86   σ Standard deviation of the distribution.

87   σ_{yield} Steel yield stress

88   τ Shear stress on the lateral surface of the bolt

89   τ_{lim} Ultimate limit shear stress of the rock-bolt interface

90   ϑ Inclination of the sliding surface with respect to the horizontal plane

91

Introduction

During underground construction of different infrastructures, stability is expected, therefore reinforcement is needed to keep the excavation stable (Pelizza et al., 2000). A number of factors affect the underground stability in joint rock masses, e.g. high rock stress, poor rock mechanical properties, excessive ground water pressure (Chen, 1994). Fully grouted passive bolts are widely used in the tunnel and underground caverns as a stabilization intervention. Many studies have been carried out to describe their behavior in rock masses considered to be homogeneous and continuous (Osgoui and Oreste, 2007; Ranjbarbia et al., 2014; 2016; Oreste, 2013). Passive rock bolt elements have a zero initial load and the mobilized stabilizing load increases with the displacement of the potentially unstable rock block. Continuously mechanically coupled (CMC) bolts rely on a curing agent (cementitious of resin grout; i.e. Spagnoli et al., 2021) that fills the annulus between the element and the borehole wall (Bawden, 2011). Rock bolts are primarily stressed by tensile and shear loads, which are caused by rock movements. The stress on the rock bolts depends on the type of rock failure (crack fracture, folding, shear fracture etc.). The essential task of the rock bolt consists in keeping the rock as stable as possible or to increase the shear resistance (Feder, 1980). Especially in tunnel construction, rock-bearing elements are in a statically undetermined system with different rock stiffness values (Blümel, 1996). Ferrero (1995) and Kilic et al. (2002) pointed out that the main factors affecting the shear and bond strength of rock bolts are the rock bolts' materials, the geometry of the bolt (bolt shape, diameter and length), type of binder, type of rock mass and fracture system. Moosavi et al. (2002) proved that a stress decrease in poor-quality rock resulted in completely ineffective bolt behavior. Therefore, any changes occurring at the bolt–grout or grout–rock interface affect the bolt bond strength and bolt load capacity.

6

117   Recently Oreste et al. (2020) used the Block Reinforcement Procedure (BRP) (Oreste

118   and Cravero, 2008; Oreste, 2009), to run a parametric analysis considering different

119   diameter of the steel bar, thickness of the binder ring around the bar, length of the bolt

120   in the unstable block, total length of the bolt, elastic modulus of the binder and

121   inclination of the sliding surface of a rock block with respect to the horizontal plane.

122   This model considers a bolt which crosses the potentially unstable block (with a length

123   L_a) and reach the stable rock behind it, where it penetrates for a certain length (L_p),
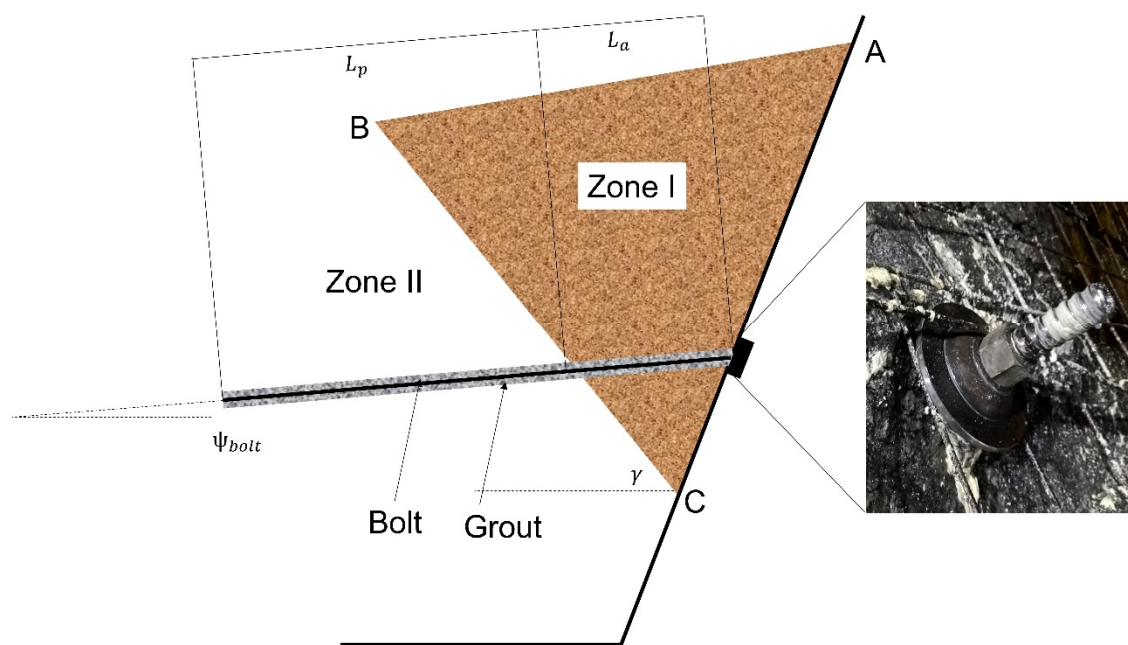
124   see Fig. 1.

125

126   **Fig. 1 Schematic representation of the potentially unstable block of rock and the**

127   **passive bolt crossing it (not to scale).**

128   The method allows to calculate the axial, N, and shear, T, forces, and the bending

129   moments M developing along the bolt, as a linear function of the (very small)

130   displacements of the block. Then the stabilizing forces, applied by the single bolt to

131   the potentially unstable block, are evaluated. The rock-bolt interaction involves the

132   presence of independent springs according to Winkler's approach, both in the

133　transverse and axial direction with respect to the bolt (Figure 2) (Oreste and Cravero,
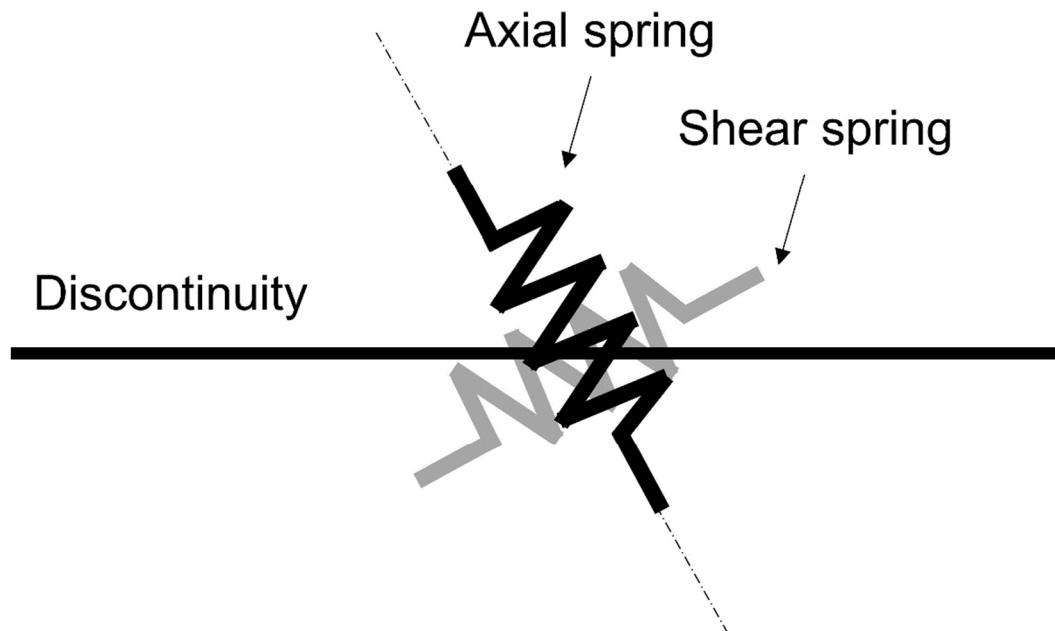
134　2008).

135

Fig. 2 Model for axial and shear springs at a discontinuity

137　The parameters influencing the interaction are difficult to evaluate, because they

138　depend on the bending and axial rigidity of the bolts, on the stiffness of the grout

139　surrounding the bar, on the stiffness of the rock at the contour of the bolt. Furthermore,

140　laboratory tests are time-consuming to carry out.

141　In addition, the forces necessary to simulate the rock-bolt interaction during

142　movements, even very small, of the potentially unstable block of rock can be

143　considerable.

144　More recently, Oreste and Spagnoli (2020) have proposed simplified equations to

145　simulate the static contribution of fully grouted bolts on potentially unstable (by sliding)

146　rock blocks, in terms of axial and transverse force to the bolt. These equations are

147　reliable even if they are based on simplifying hypotheses: the errors are negligible,

148 considering the typical range of variability of the parameters influencing the rock-bolt

149 interaction. However, the problem of the reliable definition of the parameters

150 influencing the evaluation of the stabilizing forces of the potentially unstable block of

151 rock remains.

152 This work illustrates a new probabilistic approach able to manage the uncertainty on

153 various parameters that affect the behavior of bolts and to provide the probabilistic

154 distribution of the safety factor of the rock blocks for each different stabilization

155 intervention scheme. supposed. From the results obtained, it is possible to design the

156 stabilization work, for example by defining the diameter of the bolts required, based

157 on a greater knowledge of the effects of the uncertainty of the geotechnical parameters

158 on the degree of stability of the rock blocks. The same probabilistic approach used for

159 this specific stabilization problem can be adopted in other stability problems in the

160 geotechnical field.

161 After describing the proposed probabilistic procedure in the field of geotechnical

162 engineering and of rock mechanics, the stabilization mechanisms of passive fully

163 grouted bolts on rock blocks showing a potential planar slip are illustrated. Finally, the

164 application of the probabilistic approach to a specific real case will be illustrated.

165 The authors hope that the use of a probabilistic approach such as the one illustrated

166 in this work, which does not require the use of specific software or complex

167 procedures, will allow a more correct and responsible design of the engineering

168 interventions necessary in stability problems in geotechnical engineering.

169

170 **Proposed probabilistic approach in the evaluation of the safety factors in**

171 **geotechnical engineering**

The probabilistic analysis in geotechnical engineering evaluates the probability of a certain event occurs considering certain data relating to the geotechnical properties of the system (e.g. Griffiths and Fenton, 2009). Variability of ground properties constitutes a major source of uncertainty when contending with geotechnical problems (Franco et al., 2019). The adoption of probabilistic methods relating the uncertainty of the different geotechnical properties on the final output has proven to be a valuable approach (e.g. Tang et al., 1976; Ronold and Bysveen, 1992; Oreste, 2005; Spagnoli et al., 2018; Spagnoli and Shimobe, 2020).

Several probabilistic techniques are used to account the uncertainty of the geotechnical parameters. General probabilistic methods are used to quantify the probability of occurrence of a single behavior (or property) for rocks and soils (e.g. Schubert and Goricki, 2004; Oggeri and Oreste, 2012; Mollon et al., 2013; Oreste, 2015; Spagnoli et al., 2017). More specifically, Cherubini et al. (2004), Trivedi and Zimmer (2005), Nelsen (2006), to name a few, modelled multivariate data based on the copula theory in which a copula function instead of the correlation matrix is used to represent the dependence relationship among random variables. For instance, Cao and Wang (2014), Ching et al. (2016), Zhang et al. (2014), Contreras et al. (2018), used a Bayesian method to characterize the spatial variability of soil (rock) properties, quantify the model selection uncertainty and to compare the validity of the candidate models. The point estimate method was used in geotechnical reliability analysis by Schweiger et al. (2001) and Christian and Baecher (2002).

Monte Carlo technique, which involves generating a large number of random samples from the input distributions and put into the transfer function, were investigated by Oreste (2005), Sari et al. (2010), Aladejare and Akeju (2020).

196 In the absence of more detailed information on the probabilistic distributions of the

197 parameters considered uncertain in the calculation, the normal (Gaussian) distribution

198 is used, expressed by the following equation:

199 $$f(x) = \frac{1}{\sigma \cdot \sqrt{2 \cdot \pi}} \cdot e^{-\frac{(x-\mu)^2}{2 \cdot \sigma^2}}$$ (1)

200 Where:

201 $f(x)$ is the is the probability density associated with the x value of the geotechnical or

202 geomechanical parameter considered;

203 μ is the mean value of the distribution;

204 σ is the standard deviation of the distribution.

205 The probabilistic distribution of Gauss is symmetrical and requires that 69.83% of

206 cases are included within the range $[\mu - \sigma]$- $[\mu + \sigma]$, 95.45% of cases in the interval

207 $[\mu - 2\sigma]$- $[\mu + 2\sigma]$ and 99.73% of cases in the interval $[\mu - 3\sigma]$- $[\mu + 3\sigma]$ (Fig. 3).

208 More specifically, 95% of cases are included in the range $[\mu - 1.96\sigma]$- $[\mu + 1.96\sigma]$ and

209 99% of the cases in the interval $[\mu - 2.58\sigma]$- $[\mu + 2.58\sigma]$.
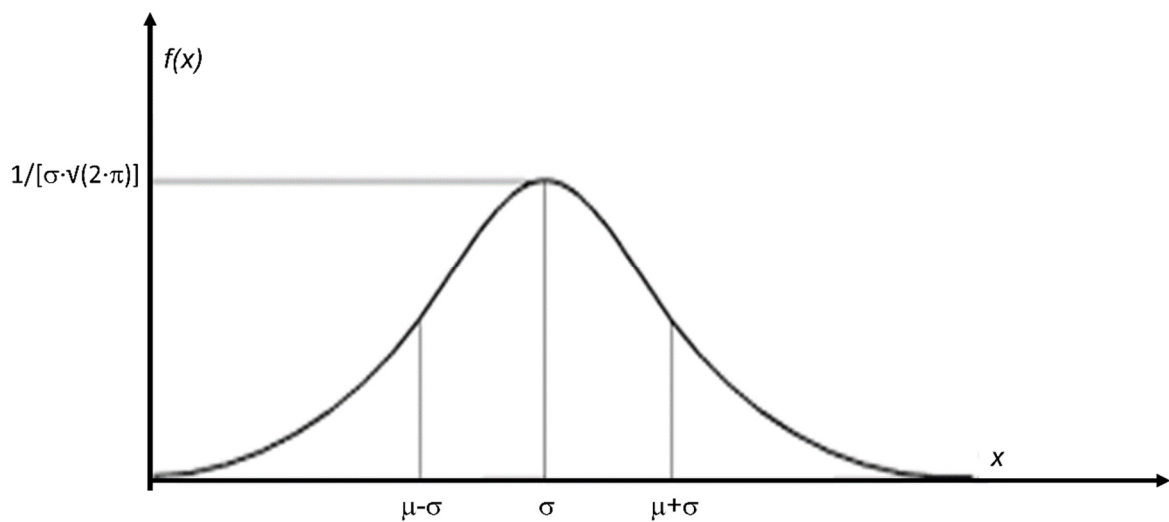
210

211 **Fig 3. Gauss probabilistic distribution trend used to represent the uncertainty**

212 **of the parameters in the geotechnical and geomechanical field.**

213   Therefore, starting from *in situ* or laboratory tests, it is possible to obtain samples of

214   measurements for each influential parameter (input data), in order to have an estimate

215   of the average values and standard deviations of the probabilistic distributions to be

216   adopted in the calculation. Alternatively, by identifying the variability interval of a

217   parameter x associated with a certain probability, p, that the real value falls within that

218   interval (for example 95% or 99%), it will be possible to determine the average value

219   μ and the standard deviation σ of the Gaussian distribution to be used in the

220   calculation:

221    $\mu = \frac{(x_{max}+x_{min})}{2}$ (2)

222    $\sigma(p = 95\ \%) = \frac{(x_{max}-x_{min})}{3.92}$ (3)

223    $\sigma(p = 99\ \%) = \frac{(x_{max}-x_{min})}{5.16}$ (4)

224   Where x_{max} and x_{min} are respectively the minimum and maximum values of the

225   variability interval of x.

226   The procedure proposed in this article provides that all parameters considered

227   uncertain are described by a probabilistic distribution, while those considered certain

228   are described by a simple representative (deterministic) value.

229   Once the probabilistic distributions of the uncertain parameters $(x_1, x_2, \dots x_i, \dots x_n,$

230   where n is the total number of parameters considered uncertain) necessary for the

231   calculation are known, it is possible to proceed with the random extraction of the values

232   by adopting the Monte Carlo procedure.

233   If it can be assumed that these parameters are independent of each other, samples of

234   m values can be created for each parameter x_i, by ordering the values thus obtained.

235   At this point m data vectors are formed $[x_1, x_2, \dots x_i, \dots x_n]_{j=1\ \text{to m}}$ with all the

236   parameters present in the same position j of the extracted sequence, with j varying

237   from 1 to m. m is the number of random extractions that are performed for each of the

238   n uncertain parameters, using the probabilistic distributions of each parameter.

239   For example, if in the problem under examination there are 5 parameters considered

240   uncertain (n = 5: x_1, x_2, x_3, x_4, x_5) and 1000 extractions are adopted with the Monte

241   Carlo procedure (m = 1000), 1000 vectors can be obtained of input data, as shown

242   below:

243   $[x_1; x_2; x_3; x_4; x_5]_{j=1}$

244   $[x_1; x_2; x_3; x_4; x_5]_{j=2}$

245   ...

246   $[x_1; x_2; x_3; x_4; x_5]_{j=999}$

247   $[x_1; x_2; x_3; x_4; x_5]_{j=1000}$

248   After having built up a sample of values extracted from the probabilistic distribution of

249   each random variable, it is possible to proceed to the determination of the safety factor

250   of the problem under examination for each series of values obtained from the different

251   extracted samples. In this way it is possible to create a sample of values of the safety

252   factor which can then be statistically treated:

253   $[x_1; x_2; x_3; x_4; x_5]_{j=1}$ $F_{S\ (j=1)}$

254   $[x_1; x_2; x_3; x_4; x_5]_{j=2}$ $F_{S\ (j=2)}$

255   ...

256   $[x_1; x_2; x_3; x_4; x_5]_{j=999}$ $F_{S\ (j=999)}$

257   $[x_1; x_2; x_3; x_4; x_5]_{j=1000}$ $F_{S\ (j=1000)}$

258   The safety factor is calculated starting from the extracted values of the uncertain

259   parameters and from the representative values for those considered certain

260   (deterministic values, kept constant in the calculation). The next paragraph illustrates

261   how to evaluate the safety factor for the problem under examination: the stability of a

262   block of rock potentially unstable due to sliding on a planar surface, in the presence of

263   a stabilization intervention with fully grouted passive bolts.

264   The result of the procedure is a sample, with a number m of safety factor values, i.e.

265    $[(F_s)_1 ; (F_s)_2 ; ... ; (F_s)_i ; ... ; (F_s)_m]$.

266   In order to have a good representation of the uncertainties present, a value of m of the

267   order of a thousand values is generally required. If there is a degree of correlation

268   between 2 or more parameters, for these we proceed to the extraction of the values

269   considering the multivariate statistics, that is, for the Gauss distribution, in addition to

270   the average value and the standard deviation of each parameter, we also consider the

271   correlation coefficients between the pairs of related parameters.

272   The analysis of the sample of the m values of the safety factor allows us to understand

273   the nature of its probabilistic distribution. Even if a Gaussian distribution is assumed

274   for each of the input data of the problem, the sample of the safety factor values in

275   general shows a probabilistic distribution different from the Gaussian one, which can

276   also have multimodal trends, such as the one shown in Figure 4.

277   It is important to check the sample of the safety factors obtained by analyzing the trend

278   of the histogram of the relative frequencies, in order to identify the theoretical

279   distribution that best represents the sample of the safety factors obtained from the

280   calculation.

281   Any confirmation of the theoretical distribution identified can then be made through the

282   Q-Q plot which compares the quantiles of the identified theoretical distribution with the

283   empirical quantiles on the sample data of the obtained safety factors.

284   The theoretical distribution that best represents the sample of safety factors allows

285   subsequently to have an indication of the probability that the safety factor is lower than

286   a certain predefined value $\overline{F_S}$. For example, it is very interesting to evaluate the

287 stability limit condition associated with a safety factor of 1 (i.e. $\overline{F_S} = 1$) and to determine

288 the probability that the safety factor is lower than this value $(F_S < \overline{F_S})$.

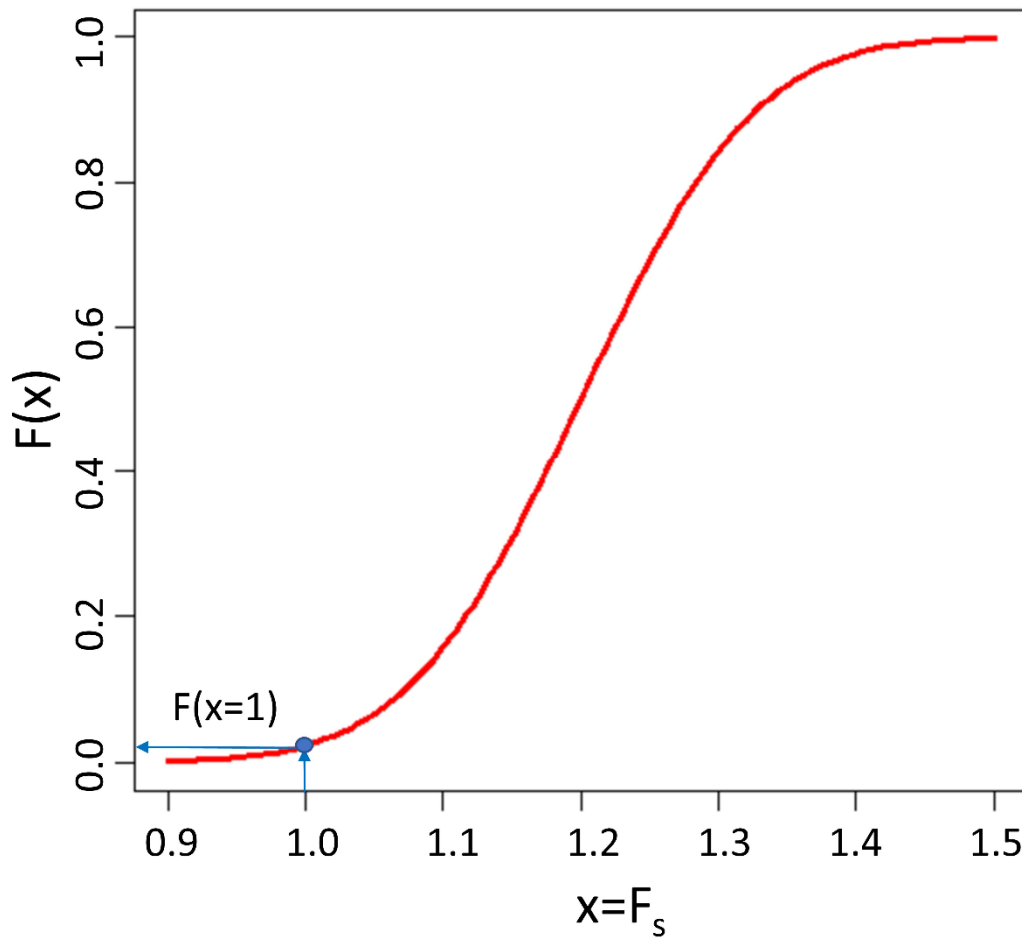289 To do this, reference is made to the cumulative distribution of probabilities (Figure 5).
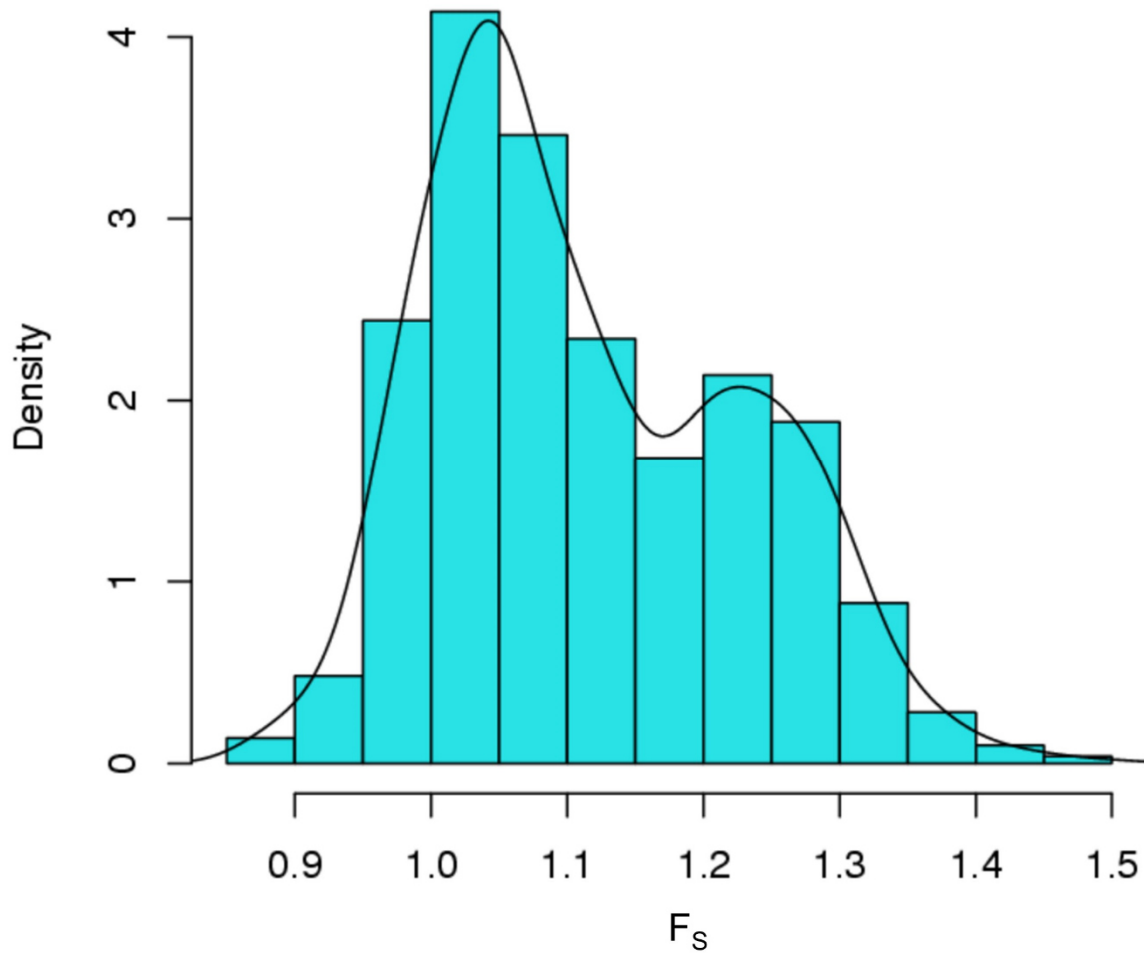
290

291 **Fig 4. General trend of the distribution of safety factors (F_S) obtained by**

292 **calculating the relative frequencies through the histogram.**

293

Fig 5. Cumulative distribution of the probabilities (Gauss curve) of the safety factor, with indication of the probability F (x = 1) that the safety factor is less than unity.

This procedure can be carried out for the geotechnical problem under examination to ensure the stability of the soil or rock in the absence and in the presence of the supports and reinforcements to be designed.

A modern approach to the design of the interventions can therefore be conducted by checking whether the probability of instability is significantly reduced to very low and acceptable values in the presence of the supports and reinforcements of the soil or rock assumed in the project.

16

305   Figure 6 shows a summary flow chart of the proposed procedure in order to to perform

306   the probabilistic analysis of the stability of a rock block in a simple and fast way in the

307   presence of the planned stabilization interventions.
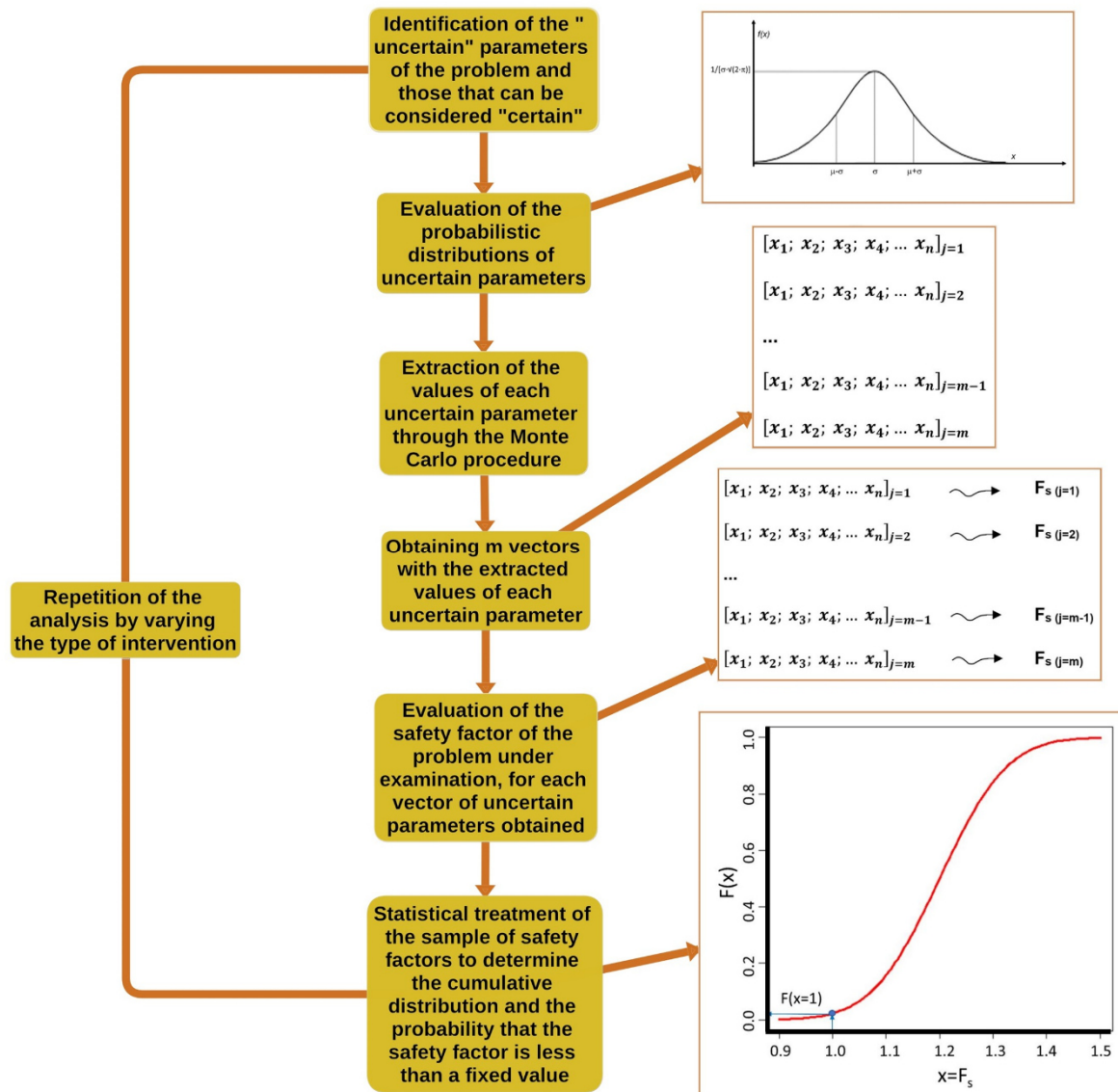
308

309   **Fig 6. Flow chart of the procedure proposed for the evaluation of the stability**

310   **conditions (through the evaluation of the safety factor) of a potentially unstable**

311   **rock block, in the presence of stabilization interventions with fully grouted**

312   **passive bolts.**

313

Model description considering the stability of a two-dimensional block of rock with regard to sliding

Fully grouted passive bolts develop internal forces linearly dependent on the displacements of the rock block that they must stabilize (Oreste and Cravero, 2008). The internal forces developed can be analyzed by referring to the interaction mechanism in the two directions perpendicular and parallel to the lateral interface of the bolt, in contact with the rock. There is a maximum displacement δ_{max} of the block for which the internal forces induce safety factors at breakage and extraction equal to the minimum ones considered admissible. The displacement δ_{max} is, therefore, to be considered as the maximum displacement of the block still compatible with the stability and efficiency of the bolt.

The shear T_0 and axial forces N_0 developing in the bolt at the point of intersection with an external surface of the block (which isolates the block from the stable rock behind) are also the stabilizing forces that the single bolt applies to the potentially unstable block. The maximum values of these forces that the bolt is able to offer to the block are obtained in correspondence with the displacement δ_{max} and are, therefore, indicated as $T_{0,\delta_{max}}$, and $N_{0,\delta_{max}}$ (Fig. 7).

Following a detailed parametric study within the typical variability ranges of the parameters influencing the bolt-rock interaction, it was possible to obtain the evaluation of the forces $T_{0,\delta_{max}}$, and $N_{0,\delta_{max}}$ that each single bolt potentially applies to the unstable block (Oreste and Spagnoli, 2020):
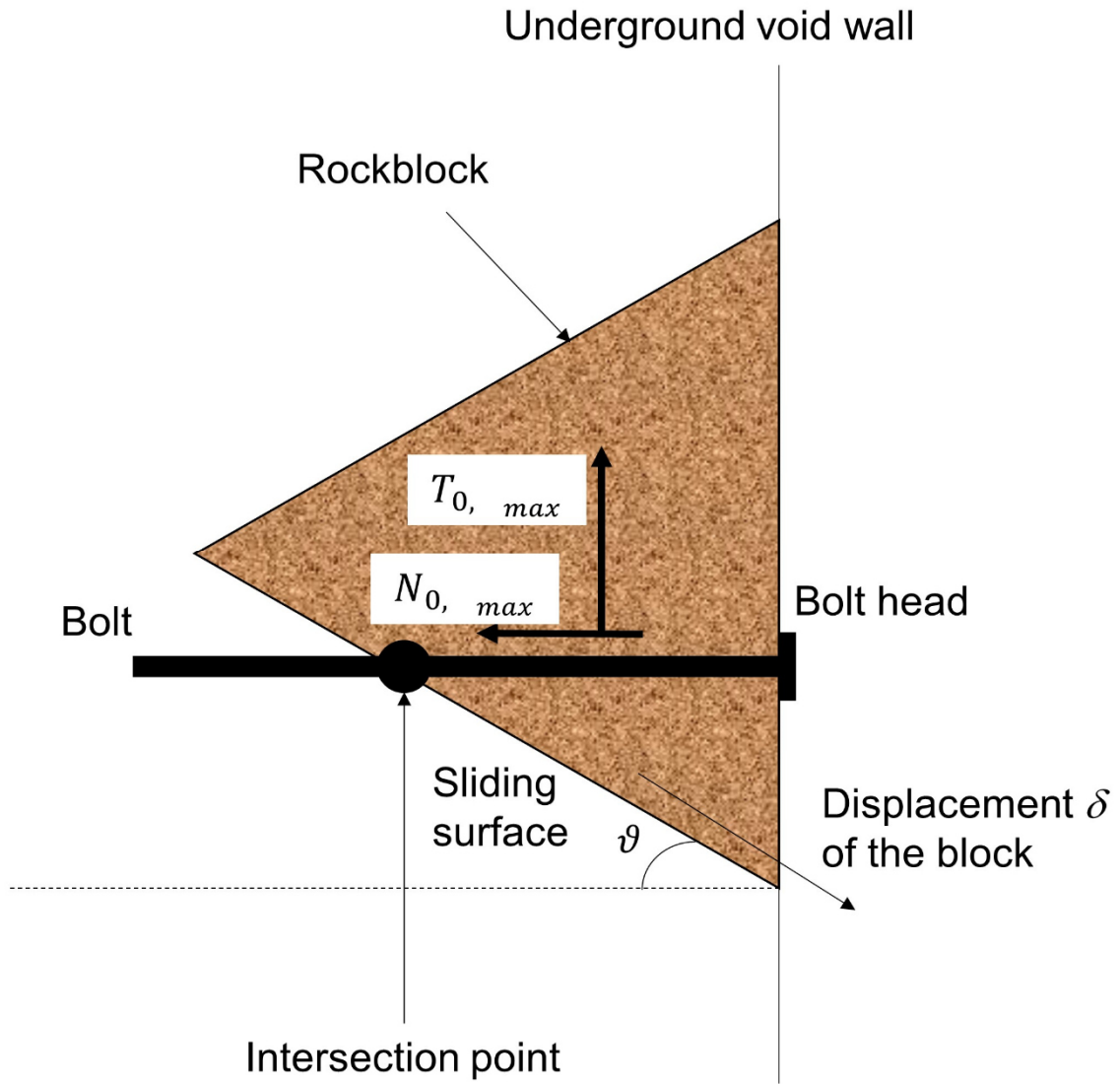
$$T_{0,\delta_{max}} = min\left(\frac{N_{yield}}{F_{s,adm,yield}} \cdot \frac{2}{\sqrt{\frac{\lambda^2 \cdot \chi^2}{tan^2(\vartheta)}+\frac{64}{3}}} \; ; \; \frac{N_{slip}}{F_{s,adm,slip}} \cdot \frac{2 \cdot tan(\vartheta)}{\lambda \cdot \psi \cdot \alpha} \right) \tag{5}$$

$$N_{0,\delta_{max}} = min\left(\frac{N_{yield}}{F_{s,adm,yield}} \cdot \frac{1}{\sqrt{1+\frac{64}{3} \cdot \frac{tan^2(\vartheta)}{\lambda^2 \cdot \chi^2}}} \; ; \; \frac{N_{slip}}{F_{s,adm,slip}} \cdot \frac{\omega}{\alpha} \right) \tag{6}$$

337   Where:

338    $\lambda = \left[\dfrac{(EA)_{bolt} \cdot \alpha}{(EJ)_{bolt} \cdot \beta^3} \right]$ (7)

339    $\chi = \left[\dfrac{\left(1 + e^{-2\alpha L a}\right) \cdot \left(1 - e^{-2\alpha L p}\right)}{\left(1 + e^{-2\alpha(L_a + L_p)}\right)} \right]$ (8)

340

341   **Fig. 7 Sketch of the stabilizing forces applied by the fully grouted passive bolt**

342   **to the potentially unstable rock block on the walls of an underground cavity (not**

343   **to scale).**

344   N_{slip} is the force which causes the bolt-rock interface to fail for a unit bolt length $N_{slip} =$

345    $\tau_{lim} \cdot \pi \cdot \Phi_{hole}$;

346   τ_{lim} is ultimate limit shear stress of the interface rock-bolt;

347   N_{yield} is the force causing the bar failure under a tensile stress $N_{yield} = \sigma_{yield} \cdot A_{bar}$;

348   σ_{yield} is the yield stress of steel;

349   A_{bar} is the area of the section of the steel bar constituting the bolt $A_{bar} = \pi \cdot \frac{\Phi_{bar}^2}{4}$;

350   J_{bar} is the moment of inertia of the steel bar constituting the bolt, $J_{bar} = \pi \cdot \frac{\Phi_{bar}^4}{64}$

351   β is the parameter that characterizes the interaction in the transversal direction

352   between bolt and rock:

353   $\beta = \sqrt[4]{\dfrac{k \cdot \Phi_{hole}}{4 \cdot (EJ)_{bolt}}}$ (9)

354   k is the ratio between the normal pressure, p, which is applied on the perimeter of the

355   bolt by the surrounding rock, and the transversal displacement, y, of the bolt;

356   α is a parameter characterizing the interaction in the axial direction between bolt and

357   rock as:

358   $\alpha = \sqrt{\dfrac{\beta_c \cdot \pi \cdot \Phi_{hole}}{(EA)_{bolt}}}$ (10)

359   $(EA)_{bolt}$ is the axial stiffness of the bolt, evaluated as:

360   $(EA)_{bolt} = E_{st} \cdot \left(\frac{\pi}{4} \cdot \Phi_{bar}^2 \right) + E_{binder} \cdot \left[\frac{\pi}{4} \cdot \left(\Phi_{hole}^2 - \Phi_{bar}^2 \right) \right]$ (11)

361   $(EJ)_{bolt}$ is the bending stiffness of the bolt, evaluated on the basis of the following

362   equation:

363   $(EJ)_{bolt} = E_{st} \cdot \left(\frac{\pi}{64} \cdot \Phi_{bar}^4 \right) + E_{binder} \cdot \left[\frac{\pi}{64} \left(\Phi_{hole}^4 - \Phi_{bar}^4 \right) \right]$ (12)

364   Φ_{bar} is the bar diameter;

365   Φ_{hole} is the diameter of the hole where the bolt is inserted as $\Phi_{hole} = \Phi_{bar} + 2 \cdot t_{binder}$;

366   t_{binder} is the thickness of the binder annulus around the steel bar;

367   E_{st} is the steel elastic modulus;

368   E_{binder} is the elastic modulus of the binder surrounding the steel bar in the hole.

369   β_c is the ratio between the shear stresses developing on the perimeter of the bolt (on

370   the wall of the hole), τ, and the relative axial displacements, v_r. β_c depends in general

371   on the characteristics of the material surrounding the steel bar and on the elastic

372   modulus of the rock;

373   L_a and L_p are respectively the lengths of the bolt inside the potentially unstable rock

374   block (zone I) and in the stable rock (zone II); their sum is the total length of the bolt.

375   The normal (k) and tangential (β_c) stiffness parameters describe the bolt-rock

376   interaction and significantly affect the behavior of the bolt. Other fundamental

377   parameters are the values of the ultimate breaking stress of the bolt-rock interface

378   (τ_{lim}) and the strength of the steel (σ_{yield}).

379   ϑ is the angle that the sliding surface of the block forms with the horizontal plane. In

380   the typical case of horizontal bolts and perpendicular to the vertical rock wall, this angle

381   is also the angle that the sliding surface forms with the direction of the bolts.

382   A detailed parametric analysis, considering the typical variability of the parameters that

383   affect the bolt-rock interaction and, therefore, the behavior of the bolts, allowed to

384   evaluate the points where the bolt can fail.

385   Thanks to the evaluation of these points (Oreste and Spagnoli, 2020), it was possible

386   to identify simple summary equations of the maximum values of the two forces ($T_{0,\delta_{max}}$

387   and $N_{0,\delta_{max}}$) which still guarantee a certain safety margin with regard to the failure of

388   the bolt in the critical points identified by the parametric analysis. The parameters

389   falling within the equations are obtained by the *in situ* tests described in some detail in

390   the next paragraph.

391   The safety factor of the block, evaluated as the ratio between the resisting forces and

392   the unstable forces, is expressed by the following equation in the presence of the

393   stabilizing forces of the bolts (in the case of horizontal bolts):

394 $$F_s = \frac{c \cdot A + \left[(W - n \cdot T_{0,max}) \cdot cos\vartheta + n \cdot N_{0,max} \cdot sin\vartheta\right] \cdot tan\varphi}{(W - n \cdot T_{0,max}) \cdot sin\vartheta - n \cdot N_{0,max} \cdot cos\vartheta}$$ (13)

395 Where:

396 c is the cohesion on the natural discontinuity which constitutes the sliding surface;

397 A is the area of the sliding surface of the block;

398 W is the weight of the potentially unstable rock block;

399 n is the number of fully grouted passive bolts present;

400 φ is the friction angle on the natural discontinuity constituting the sliding surface.

401

402 This equation reports at the numerator the stabilizing forces, which oppose the

403 movement of the block, evaluated in the direction of sliding (i.e. the line of maximum

404 slope on the sliding surface); the denominator includes the unstable forces, those that

405 tend to move the block, also evaluated in the direction of sliding of the block.

406 This equation permits to proceed with the design of the bolts through the choice of the

407 solution that allows to obtain the safety factor of the desired rock block. It is possible

408 to proceed by trial and error, changing the geometric characteristics of the bolt

409 (dimensions of the steel bar and of the entire bolt, length of the bolt) and the number

410 of bolts, until the block is stabilized, with a safety margin considered acceptable.

411

412 **Application of the probabilistic approach to a real case**

413 There are several parameters influencing the safety factor of a rock block considering

414 fully grouted passive bolts:

415 • cohesion and friction angle of the discontinuity representing the sliding surface;

416 • weight of the rock block, which is function of the volume and the specific weight

417 of the rock;

418 • geometry of the bolts (of the steel bar and of the grout surrounding it);

419   •   stiffness parameters of the bolt-rock interaction on the interface at the lateral

420   surface of the bolt;

421   •   strength of the bolt-rock interface to bolt extraction;

422   •   tensile strength of the steel constituting the bolt bar;

423   •   elastic modulus of the steel and of the grout around the bar.

424 Several of these parameters are usually known only with some accuracy. In particular,

425 there are often large uncertainties on the stiffness parameters characterizing the

426 interaction between bolts and rock (k and β_c), on the strength of the bolt-rock interface

427 to bolt extraction (τ_{lim}), as well as on the cohesion (c) and friction angle (φ) of the

428 natural discontinuity representing the sliding surface. Specific laboratory tests are

429 carried out in order to evaluate these parameters, but from the tests it is possible to

430 obtain values that are often not very representative because the results can be

431 dispersive and the number of tests is generally limited.

432 To obtain the estimate of the cohesion and the angle of friction of the sliding surface,

433 shear tests are carried out on rock samples at the laboratory scale; to evaluate the

434 stiffness parameters of the bolt-rock interaction, specific load tests are prepared *in situ*

435 both in the axial and transverse direction of the bolt (Oreste and Spagnoli, 2020). To

436 determine the shear strength of the bolt-rock interface, we use the results pull-out tests

437 of a *in situ* test bolt with the application of a force in the axial direction.

438 The uncertainty about the evaluation of these parameters cannot be represented

439 simply by an average value of the results of *in situ* and laboratory tests. It is more

440 appropriate to consider a range of variability for uncertain parameters and associate it

441 to a certain probability that the real value falls within this range.

442 Such an approach was adopted to study the stabilization intervention of a block of

443 limestone potentially unstable due to flat sliding on a natural discontinuity with an

444   inclination of 35° with the horizontal plane (Oreste and Spagnoli, 2020). This

445   potentially unstable block, located on a municipal road in the northern part of Piedmont

446   (Italy), was analyzed to verify the need for a stabilization intervention with fully grouted

447   passive bolts and to design the intervention. Specific *in situ* and laboratory tests have

448   been developed.

449   The *in situ* tests on test bolts made it possible to obtain the stiffness coefficients of the

450   normal (k) and transverse (β_c) interaction of 8.90 ± 1.20 MPa/mm and 1.18 ± 0.38

451   MPa/mm respectively, with a confidence level of each variability interval greater than

452   99%.

453   The pull-out tests provided a stress limit of 2.08 ± 0.73 MPa. The shear tests

454   developed in the laboratory on samples including natural discontinuity, allowed to

455   determine the values of cohesion and friction angle of the sliding surface: c = 8.0 ± 2.3

456   kPa and φ = 23.0 ° ± 1.40 °.

457   Assuming the mutual independence of the identified random variables and also

458   assuming a normal distribution (Gaussian probabilistic distribution), it is possible to

459   obtain the probabilistic distribution of each uncertain parameter and in particular the

460   standard deviation as well as the average value already known:

461   - cohesion c of the sliding surface: $\bar{x}_c$=8.0 kPa; σ_c=0.89147 kPa

462   - friction angle φ of the sliding surface: $\bar{x}_\varphi$=23.0 °; σ_φ=0.54264 °

463   - stiffness parameter β_c in the bolt-rock shear interaction: $\bar{x}_{\beta c}$=1.18 MPa/mm;

464      $\sigma_{\beta c}$=0.14729 MPa/mm

465   - stiffness parameter k in the normal bolt-rock interaction: $\bar{x}_k$=8.90 MPa/mm;

466   σ_k=0.46512 MPa/mm

467   - limit shear stress on the bolt-rock interface: $\bar{x}_{\tau lim}$=2.08 MPa; $\sigma_{\tau lim}$=0.28295 MPa.

468   The standard deviation was assumed to be $\frac{1}{5.16}$ of the width of the variability interval,

469   associating the latter with a confidence level of 99%.

470   The calculation of the safety factor F_S in the presence of some random variables can

471   be performed with the Monte Carlo method. After having built up a sample of values

472   extracted from the probabilistic distribution of each random variable, it is possible to

473   proceed to the determination of the safety factor for each series of values obtained

474   from the different extracted samples. In this way it is possible to create a sample of

475   values of the safety factor which can then be statistically treated.

476   If, for example, the number of the values of each sample obtained is m, it will be

477   possible to constitute m data series of the random variables, represented as follows:

478    $[(c)_1; (\varphi)_1 ; (\beta_c)_1; (k)_1; (\tau_{lim})_1]$

479    $[(c)_i ; (\varphi)_i ; (\beta_c)_i ; (k)_i ; (\tau_{lim})_i]$

480    $[(c)_m ; (\varphi)_m ; (\beta_c)_m ; (k)_m ; (\tau_{lim})_m]$

481

482   The result is a sample, with a number m, of safety factor values:

483    $[(F_s)_1 ; (F_s)_2 ; \dots ; (F_s)_i ; \dots ; (F_s)_m]$

484   The remaining parameters affecting the calculation of the safety factor were

485   considered known with an acceptable accuracy and remain constant during the

486   calculation:

487   • inclination ϑ of the sliding surface with respect to the horizontal plane: 35°;

488   • sliding surface area A: 10 m²;

489   • weight W of the block: 1080 kN;

490   • thickness of the grout ring t_{binder} around the steel bar: 0.01 m;

491   • length of the bolt inside the rock block L_a: 1.5 m;

492   • length of the bolt in the stable rock L_p: 2.5 m;

493 • elastic modulus of steel E_{st}: 210000 MPa;

494 • elastic modulus of the cementitious grout E_{binder}: 25000 MPa;

495 • yield strength of steel σ_{yield}: 400 MPa;

496 • safety factors required with regard to the failure of the bar $F_{s,adm,yield}$ and the

497 pull-out strength of the bolt-rock interface $F_{s,adm,slip}$: 1.25.

498 These parameters are considered for the evaluation of the safety factor of the block in

499 a deterministic way, with a value remaining constant in the calculation.

500 In natural conditions, without the effect of the stabilization intervention, the safety

501 factor was found to be 0.735 and, therefore, not sufficient to guarantee the stability of

502 the block.

503 To stabilize the rock block, it was decided to adopt two fully grouted passive bolts (n

504 = 2) with steel bars of ranging from diameter Φ_{bar} = 20 mm to diameter Φ_{bar}= 26 mm.

505 From the simple deterministic analysis considering the midpoint of the intervals of the

506 uncertain parameters it is possible to obtain the safety factor trend shown in Figure 7.

507 According to this approach, all the parameters present in the calculation take on a

508 constant (deterministic) value.

509 The traditional approach should involve setting the desired safety factor and obtaining

510 the smallest diameter of the bar able to achieve this value, using the graph in Fig. 8.

511
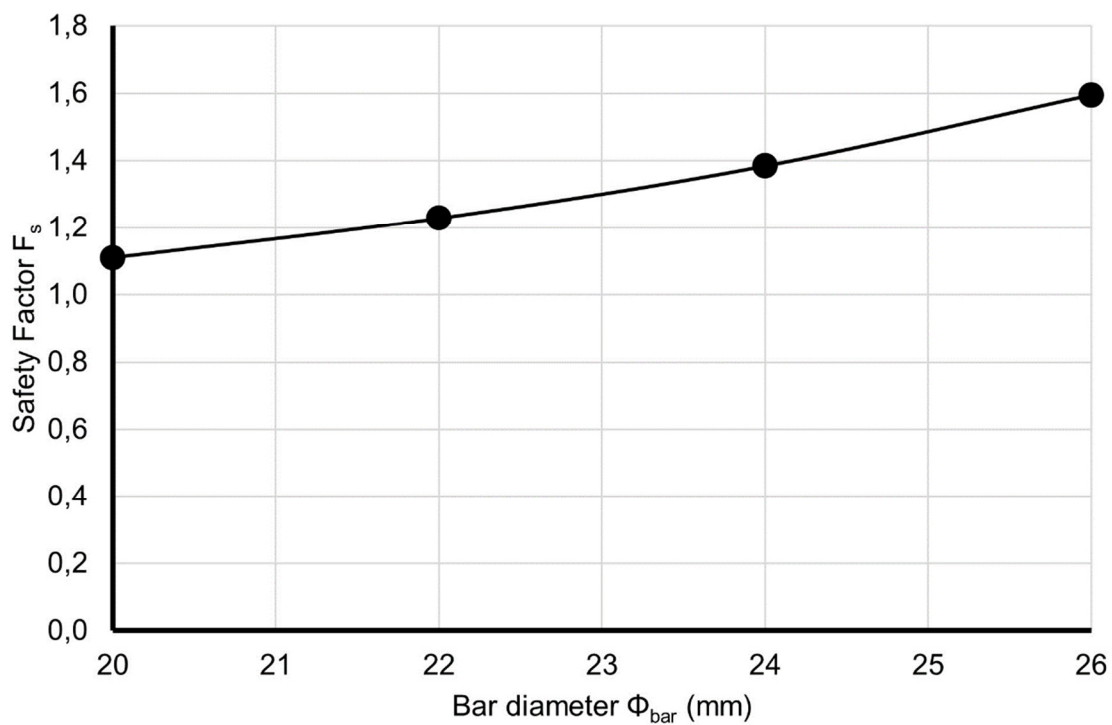
Fig. 8. Trend of the safety factor of the block as the diameter of the steel bars change, based on a deterministic analysis of the safety factors, assuming the average value of the variability intervals of each as a representative value of the parameters considered uncertain.

A subsequent and more in-depth probabilistic analysis using the Monte Carlo simulation allowed to obtain a different sample of the safety factors for each of the considered diameters. In total, therefore, 4 different samples, each consisting of thousand values of safety factors (m = 1000).

The Monte Carlo simulation is time consuming, even if for the proposed procedure the calculations proceeds rapidly, and the final solution is reached in a very limited time. The m value to be adopted depends on the stabilization of the safety factor sample. It is necessary to continuously analyze the mean and standard deviation values of this sample until these values change significantly as the number of extractions increases and, therefore, as m increases.

526 Figure 9 shows the cumulative frequencies values for each of the 4 safety factor

527 samples obtained with the Monte Carlo simulation. After the verification of the

528 probabilistic distribution closest to the obtained samples, developed through traditional

529 analysis systems, it was possible to adopt the normal distribution of Gauss (Figures

530 10-12).

531 The comparison between the sample of safety factors and the theoretical distributions

532 available was made in relation to the cumulative frequencies, the Q-Q plot and the Box

533 Plot. Figures 10-12 show the comparisons adopting the normal distribution. Since the

534 comparison gave positive results, no further comparisons were made with other

535 different theoretical probabilistic distributions.
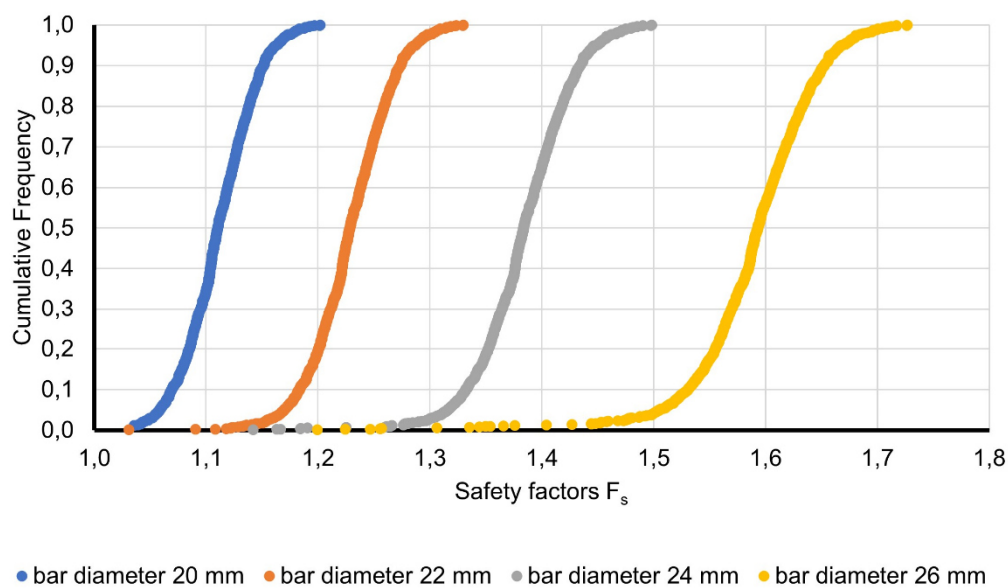
● bar diameter 20 mm   ● bar diameter 22 mm   ● bar diameter 24 mm   ● bar diameter 26 mm

536

537 **Fig. 9. Trends of the cumulative frequencies of the safety factor samples**

538 **obtained from the calculation with the Monte Carlo procedure for the 4**

539 **diameters of the bars considered: 20 mm (blue), 22 mm (orange), 24 mm (grey)**

540 **and 26 mm (yellow).**

541
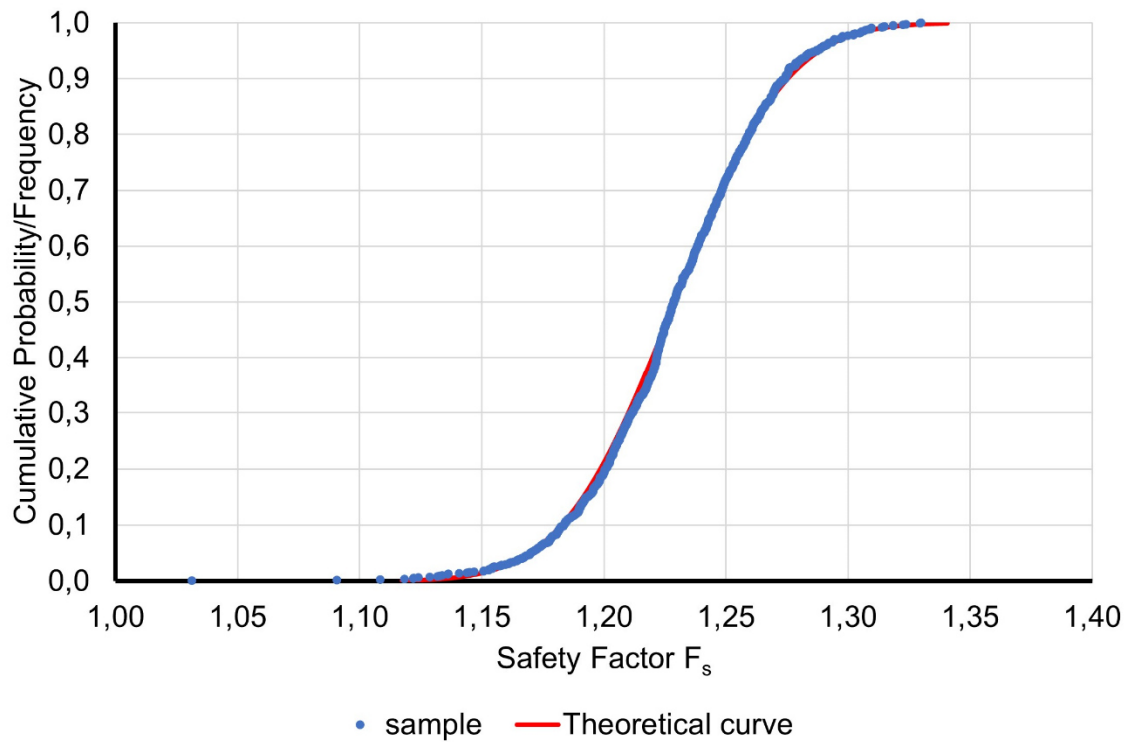
Fig. 10. Verification of the distribution of safety factors for the case of a bar diameter of 22 mm (Φ_{bar} = 22 mm) by comparing the cumulative sample frequencies and the theoretical curve of the cumulative Gaussian distribution.
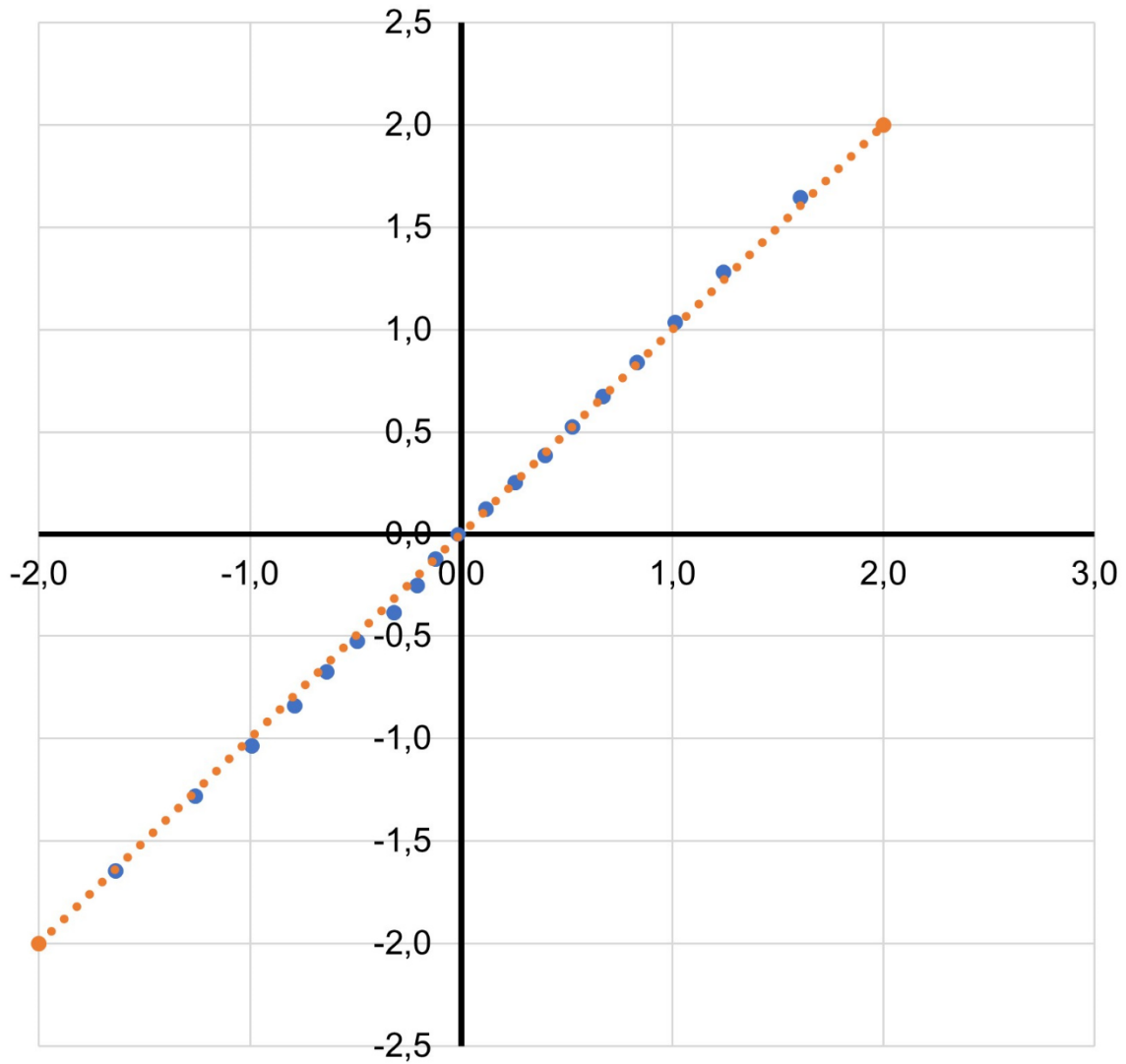
545

546

Fig. 11. Verification of the distribution of safety factors for the case of a bar diameter of 22 mm (Φ_{bar} = 22 mm) by examining the Q-Q plot relative to the comparison of the sample distribution with the theoretical curve of the cumulative distribution of Gauss .
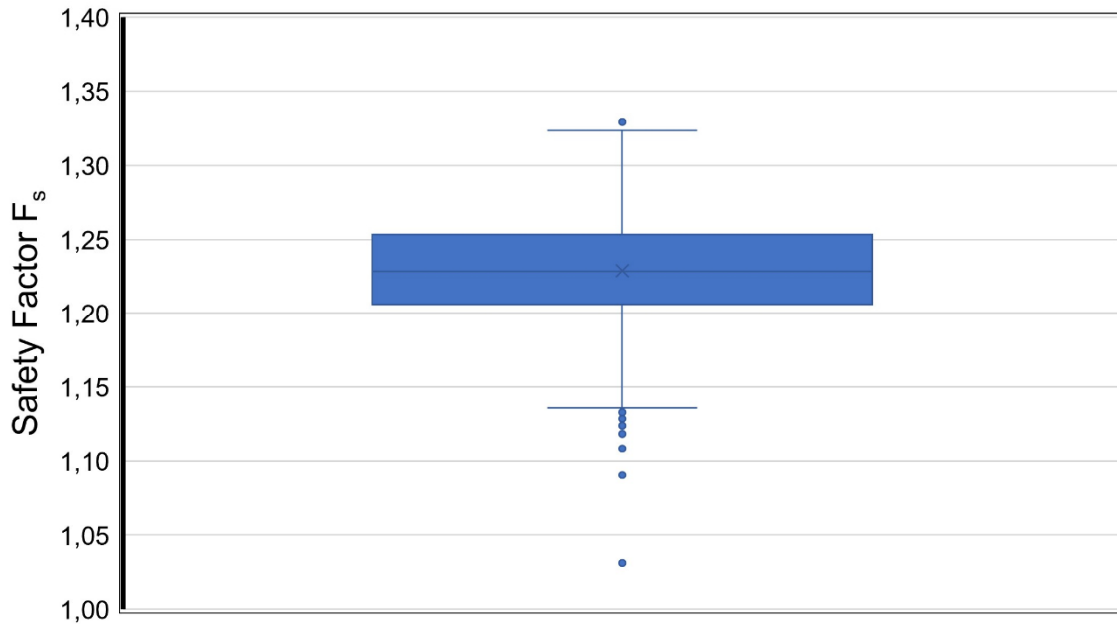
547

548

549

550

551

552

553

554

555

Fig. 12. Verification of the characteristics of the sample of safety factors for the case of a bar diameter of 22 mm (Φ_{bar} = 22 mm) by examining the Box Plot.

After the verification of the samples allowed to consider the Gaussian normal probabilistic distribution as representative, it was possible to plot the cumulative probability curves for each diameter of the bar considered, referring to the mean values and standard deviations obtained for each sample:

Φ_{bar}=20 mm: $\bar{x}_{FS}$=1.111 ; σ_{FS}=0.032

Φ_{bar}=22 mm: $\bar{x}_{FS}$=1.229 ; σ_{FS}=0.036

Φ_{bar}=24 mm: $\bar{x}_{FS}$=1.383 ; σ_{FS}=0.043

Φ_{bar}=26 mm: $\bar{x}_{FS}$=1.590 ; σ_{FS}=0.057

Thanks to the cumulative probability curves adopting the normal distribution, it is possible to evaluate, for each bar diameter, what is the probability that the safety factor is lower than a predetermined value. These probability values can be summarized in a graph as the one shown in Fig. 13. It is, therefore, possible to obtain, for example,

571   the indication to use a bar diameter equal to 24 mm to have a probability of only $1 \cdot 10^-$

572   ^{5} that the safety factor of the block is lower to 1.2.

573   It is possible therefore to obtain information of a probabilistic nature on the safety

574   factors of a block of rock starting from the degree of uncertainty on the fundamental

575   parameters of the problem under consideration, for each different diameter of the bar

576   used. Such an approach, therefore, permits to consciously design the extent of the

577   instability risks of a block of rock even in the presence of the stabilization intervention

578   to be adopted, allowing for a modern and effective design of the interventions.
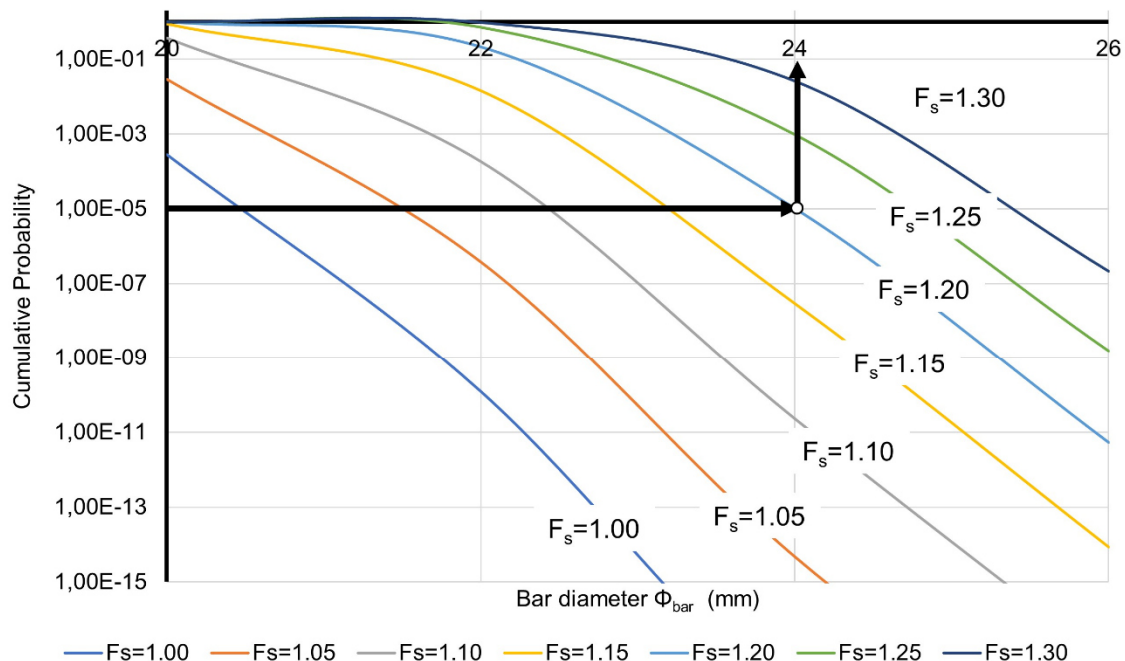
579

580   **Fig. 13. Cumulative probability as the diameter of the bar varies for different**

581   **values of the rock block safety factor. The graph permits to appropriately define**

582   **the diameter of the bar necessary to allow having a predetermined probability**

583   **that the safety factor is lower than a given value. In the example shown, it is**

584   **possible to identify a bar diameter of 24 mm in order to limit the probability that**

585   **the safety factor is less than 1.2 to 1 case in 100 thousand ($1 \cdot 10^{-5}$).**

586   The probability values were obtained with reference to a normal probabilistic

587   distribution, having the value of the mean and standard deviation equal to those of the

588   sample of safety factors obtained from the Monte Carlo simulation.

589   **Conclusions**

590   The stabilization of a block of rock on the walls of an underground cavity is usually

591   done through fully grouted passive bolts. The interaction mechanism between these

592   bolts and the surrounding rock is complex and is established only with a movement,

593   even if imperceptible, of the rock block.

594   Oreste and Cravero (2008) developed a calculation procedure for the evaluation of the

595   stabilization forces of passive bolts fully grouted on potentially unstable rock blocks.

596   More recently Oreste and Spagnoli (2020) identified some simplified formulas for the

597   definition of the stabilization forces of grouted passive bolts. However, the parameters

598   influencing the behavior of fully grouted passive bolts and leading to identify the extent

599   of the stabilization forces applied to potentially unstable blocks, are difficult to evaluate

600   and require specific laboratory tests or tests *in situ*. Such tests can be carried out only

601   in a limited number and often the results obtained are dispersive. Rather than precise

602   deterministic values, it is possible to estimate ranges of variability of the parameters

603   involved in the calculation.

604   A probabilistic approach is therefore necessary, which, starting from the uncertainties

605   of the parameters governing the bolt-rock interaction problem, leads to an assessment

606   of the possible variability of the safety factor of the rock block in the presence of

607   stabilization interventions.

608   In this article, a probabilistic approach has been proposed which is able to allow the

609   correct design of the passive fully grout bolts starting from the uncertainties on the

610   fundamental parameters of the bolt-rock interaction and on the resistance parameters

611 of the sliding surface of the block consisting of a natural discontinuity. This approach

612 is based on the Monte Carlo procedure and allows to obtain samples of the safety

613 factors for each different diameter of the steel bars of the bolts.

614 From the probabilistic analysis of these samples it was, therefore, possible to design

615 the steel bars considering the probability that the safety factor of the block with regard

616 to instability due to slipping is lower than a predetermined limit. In this way it is possible

617 to design a stabilization intervention by exploiting all the knowledge available on the

618 physical-mechanical phenomenon studied, including those relating to the uncertainty

619 of the fundamental parameters of the problem.

620 The proposed approach was applied with reference to a real case of a potentially

621 unstable rock block due to planar sliding on a natural discontinuity. The definition of

622 the diameter of the steel bars used for the stabilization intervention was obtained by

623 imposing that the block of rock may have a safety factor lower than 1.2 only for one

624 case out of one hundred thousand ($1 \cdot 10^{-5}$).

625 **Conflict of interests**

626 Authors declare they have no conflict of interest.

627 **References**

628 Aladejare AE, Akeju VO. Design and sensitivity analysis of rock slope using Monte

629 Carlo simulation. Geotech Geol Eng 2020; 38:573–585,

630 https://doi.org/10.1007/s10706-019-01048-z.

631 Bawden FW. Ground Control Using Cable and Rock Bolting. In: Darling P, editor. SME

632 Mining Engineering Handbook, Society for Mining, Metallurgy and Exploration Inc.,

633 Littleton; 2011. p. 616-617.

634 Blümel M. Untersuchungen zum Tragverhalten vollvermörtelter Felsbolzen im

635 druckhaften Gebirge. PhD thesis, Technical University, Graz, Austria; 1996.

636 Cao Z, Wang Y. Bayesian approach for probabilistic site characterization using cone

637 penetration tests. J Geotech Geoenviron Eng 2013; 139 (2):267–276.

638 Chen, D. Design of rock bolting systems for underground excavations. PhD thesis,

639 University of Wollongong, Australia; 1994.

640 Cherubini U, Luciano E, Vecchiato W. Copula Methods in Finance. Wiley, Chichester.

641 UK, 2004:

642 Ching J, Wu SS, Phoon KK. Statistical characterization of random field parameters

643 using frequentist and Bayesian approaches. Can Geotech J 2016, 53 (2). 285–298.

644 Christian J, Baecher GB. The point‑estimate method with large numbers of variables.

645 Int J Numer Anal Meth Geomech 2002, 26(15):1515-1529.

646 Contreras, LF, Brown, ET, Ruest M. Bayesian data analysis to quantify the uncertainty

647 of intact rock strength. J Rock Mech. Geotech 2018, 10.11-31

648 Feder G. Zur Wirkungsweise und Gestaltung voll eingemörtelter Stabanker. Tunnel

649 1980; 2: 98–111.

650 Ferrero M. The shear strength of reinforced rock joints. Int. J. Rock Mech. Min. Sci.

651 Geomech. Abstr 1995; 32: 595-605.

652 Franco VH, Gitirana Jr, GFN, de Assis AP. Probabilistic assessment of tunneling-

653 induced building damage. Comput Geotech 2019; 113: 103097,

654 *https://doi.org/10.1016/j.compgeo.2019.103097*.

655 Griffiths, DV, Fenton, GA. Probabilistic settlement analysis by stochastic and random

656 finite-element methods. J Geotech Geoenviron Eng 2009; 135, 11: 1629-1637.

657 Kilic A, Yasar E, Celik, AG. Effect of grout properties on the pull-out load capacity of

658 fully grouted rock bolt. Tunn Undergr Space Technol 2002; 17: 355–362.

659 Mollon, G, Dias, D, Soubra, AH. Probabilistic analyses of tunneling-induced ground

660 movements. Acta Geotech 2013; 8:181–199, DOI 10.1007/s11440-012-0182-7.

661 Moosavi M, Bawden, WF, Hyett AJ. Mechanism of bond failure and load distribution

662 along fully grouted cable-bolts. Mining Technology 2002; 111:1-12.

663 Nelsen RB. An Introduction to Copulas, 2nd ed. Springer, New York; 2006.

664 Oggeri C, Oreste P. Tunnel static behavior assessed by a probabilistic approach to

665 the back-analysis. Am J Appl Sci 2012; 9(7): 1137-1144.

666 Oreste, P. A probabilistic design approach for tunnel supports. Comp Geotech 2005;

667 32:520–534.

668 Oreste PP. Face stabilisation of shallow tunnels using fibreglass dowels. P I Civil Eng

669 Geotec 2009; 162 (2):95–109, doi: 10.1680/geng.2009.162.2.95.

670 Oreste P. Face stabilization of deep tunnels using longitudinal fibreglass dowels. Int J

671 Rock Mech Min Sci 2013; 58:127-140.

672 Oreste, PP, Cravero, M. An analysis of the action of dowels on the stabilization of rock

673 blocks on underground excavation walls. Rock Mech Rock Eng 2008; 41(6): 835–868,

674 DOI 10.1007/s00603-008-0162-2.

675 Oreste P, Spagnoli G. A simplified mathematical approach for the evaluation of the

676 stabilizing forces applied by a passive cemented bolt to a sliding rock block. Tunn

677 Undergr Space Technol 2020; 103: 103459,

678 *https://doi.org/10.1016/j.tust.2020.103459*

679 Oreste P. Analysis of the tunnel-support Interaction through a probabilistic approach.

680 Am J Appl Sci 2015; 12(2): 121.129.

681 Oreste P, Spagnoli G, Buccoleri AG. A parametric analysis on the influence of the

682 binder characteristics on the behaviour of passive rock bolts with the Block

683 Reinforcement Procedure. Geotech Geol Eng 2020; 38:4159–4168

684 https://doi.org/10.1007/s10706-020-01285-7.

685 Osgoui RR, Oreste P. Convergence-control approach for rock tunnels reinforced by

686 grouted bolts, using the homogenization concept. Geotech Geol Eng 2007; 25(4):431-

687 440.

688 Pelizza S, Oreste P, Peila D, Oggeri C. Stability analysis of a large cavern in Italy for

689 quarrying exploitation of a pink marble. Tunn Undergr Space Technol 2000; 15(4):

690 421-435.

691 Ranjbarbia M, Fahimifar A, Oreste P. Practical method for the design of pretensioned

692 fully grouted rockbolts in tunnels. Int. J. Geomec 2016; 16(1): 04015012.

693 Ranjbarbia M, Fahimifar A, Oreste P. A simplified model to study the behavior of pre-

694 tensioned fully grouted bolts around tunnels and to analyze the more important

695 influencing parameters. J Min Sci 2014; 50(3): 533-548

696 Ronold KO, Bysveen S. Probabilistic stability analysis for deep-water foundations. J

697 Geotech Eng Div ASCE 1992; VI18(3): 394-405.

698 Sari M, Karpuz C, Ayday C. Estimating rock mass properties using Monte Carlo

699 simulation: Ankara andesites. Comput and Geosci 2010;36: 959–969.

700 doi:10.1016/j.cageo.2010.02.001.

701   Schubert W, Goricki A. Probabilistic assessment of rock mass behaviour as basis for

702   stability analyses of tunnels. In: Proc. Rock Mechanics Meeting, Stockholm, Sweden,

703   March 2004, 1-20, SvBeFo.

704   Schweiger HF, Thurner R, Pöttler R. Reliability analysis in geotechnics with

705   deterministic finite elements—theoretical concepts and practical application. Int J

706   Geomech 2001; 1(4):389-413.

707   Spagnoli G, Sridharan S, Oreste P, Di Matteo L. A probabilistic approach for the

708   assessment of the influence of the dielectric constant of pore fluids on the liquid limit

709   of smectite and kaolinite. Appl Clay Sci 2017; 145:37-43.

710   *https://doi.org/10.1016/j.clay.2017.05.009*.

711   Spagnoli G, Tsuha CHC, Oreste P, Mendez Solarte CM. A sensitivity analysis on the

712   parameters affecting large diameter helical pile installation torque, depth and

713   installation power for offshore applications. DFI Journal 2018; 12(3): 171-185.

714   *https://doi.org/10.1080/19375247.2019.1595996*.

715   Spagnoli G, Shimobe S. Statistical analysis of some correlations between

716   compression index and Atterberg limits. Env Earth Sci 2020; 79(24): 532.

717   10.1007/s12665-020-09272-0.

718   Spagnoli G, Carnelli, D, Wyink U, Herrmann C. Laboratory tests of fully grouted bolts

719   with a pumpable thixotropic resin. In: Barla M, Di Donna A, Sterpi D, editors.

720   Challenges and Innovations in Geomechanics. Springer International Publishing;

721   2021; Vol. 2: 1-8. https://doi.org/10.1007/978-3-030-64518-2_103 (in press).

722   Tang W, Yucemen M, Ang AS. Probability-based short term design of soil slopes. Can

723   Geotech J 1976; 13(3): 201–215.

724   Trivedi PK, Zimmer DM.Copula modeling: an introduction for practitioners. Found.

725   Trends Financ 2005; 1 (1): 1–111.

726   Zevgolis IE, Daffas ZA. System reliability assessment of soil nail walls. Comp Geotech

727   2018; 98, 232–242.

728   Zhang J, Huang HW, Juang CH, Su WW. Geotechnical reliability analysis with limited

729   data: Consideration of model selection uncertainty. Eng Geol 2014; 181:27–37.

730   *https://doi.org/10.1016/j.enggeo.2014.08.002*

731

FIGURE CAPTION

733   **Fig. 1 Schematic representation of the potentially unstable block of rock and the**

734   **passive bolt crossing it (not to scale).**

735   **Fig. 2 Model for axial and shear springs at a discontinuity**

736   **Fig 3. Gauss probabilistic distribution trend used to represent the uncertainty**

737   **of the parameters in the geotechnical and geomechanical field.**

738   **Fig 4. General trend of the distribution of safety factors (F_S) obtained by**

739   **calculating the relative frequencies through the histogram.**

740   **Fig 5. Cumulative distribution of the probabilities (Gauss curve) of the safety**

741   **factor, with indication of the probability F (x = 1) that the safety factor is less**

742   **than unity.**

743   **Fig 6. Flow chart of the procedure proposed for the evaluation of the stability**

744   **conditions (through the evaluation of the safety factor) of a potentially unstable**

745   **rock block, in the presence of stabilization interventions with fully grouted**

746   **passive bolts.**

747   **Fig. 7 Sketch of the stabilizing forces applied by the fully grouted passive bolt**

748   **to the potentially unstable rock block on the walls of an underground cavity (not**

749   **to scale).**

750   **Fig. 8. Trend of the safety factor of the block as the diameter of the steel bars**

751   **change, based on a deterministic analysis of the safety factors, assuming the**

752   **average value of the variability intervals of each as a representative value of the**

753   **parameters considered uncertain.**

754   **Fig. 9. Trends of the cumulative frequencies of the safety factor samples**

755   **obtained from the calculation with the Monte Carlo procedure for the 4**

756　diameters of the bars considered: 20 mm (blue), 22 mm (orange), 24 mm (grey)

757　and 26 mm (yellow).

758　Fig. 10. Verification of the distribution of safety factors for the case of a bar

759　diameter of 22 mm (Φ_{bar} = 22 mm) by comparing the cumulative sample

760　frequencies and the theoretical curve of the cumulative Gaussian distribution.

761　Fig. 11. Verification of the distribution of safety factors for the case of a bar

762　diameter of 22 mm (Φ_{bar} = 22 mm) by examining the Q-Q plot relative to the

763　comparison of the sample distribution with the theoretical curve of the

764　cumulative distribution of Gauss .

765　Fig. 12. Verification of the characteristics of the sample of safety factors for the

766　case of a bar diameter of 22 mm (Φ_{bar} = 22 mm) by examining the Box Plot.

767　Fig. 13. Cumulative probability as the diameter of the bar varies for different

768　values of the rock block safety factor. The graph permits to appropriately define

769　the diameter of the bar necessary to allow having a predetermined probability

770　that the safety factor is lower than a given value. In the example shown, it is

771　possible to identify a bar diameter of 24 mm in order to limit the probability that

772　the safety factor is less than 1.2 to 1 case in 100 thousand ($1 \cdot 10^{-5}$).

773